Facile Route to Zn-Based II−VI Semiconductor Spheres, Hollow Spheres, and Core/Shell Nanocrystals and Their Optical Properties

Jun Geng,[†,‡] Bo Liu,[†] Lang Xu,[†] Fang-Neng Hu,[†] and Jun-Jie Zhu*[,†]

Key Laboratory of Analytical Chemistry for Life Science, School of Chemistry and Chemical Engineering, Nanjing University, Nanjing 210093, PR China, and Department of Chemistry, Jiangsu Institute of Education, Nanjing 210013, PR China

Received May 4, 2007. In Final Form: June 27, 2007

A convenient chemical conversion method that allows the direct preparation of nanocrystalline ZnE (E = O, S, Se) semiconductor spheres and hollow spheres as well as their core/shell structures is reported. By using monodisperse ZnO nanospheres as a starting reactant and in situ template, ZnS, ZnSe solid and hollow nanospheres, and ZnO/ZnS and ZnO/ZnSe core/shell nanostructures have been obtained through an ultrasound-assisted solution-phase conversion process. The formation mechanism of these nanocrystals is connected with the sonochemical effect of ultrasound irradiation. The photoluminescence and electrogenerated chemiluminescence properties of the as-prepared nanocrystals were investigated.

Introduction

During the past decade, a considerable effort has been spent in the preparation and investigation of wide-band-gap II−VI nanoscale semiconductors because of their fundamental electronic and optical properties.[1] Among them, Zn-based II−VI semiconductors (ZnE, E = O, S, Se, Te) have been the subject of intense interest because of their potential wide-ranging applications in pigments, gas sensors, varistors, photonic crystal devices, and short-wavelength optoelectronic devices.[2−4] The wide band gaps of ZnO, ZnS, and ZnSe also make them ideal choices as inorganic passivation shells for a variety of semiconductor core/shell nanocrystals in order to improve the stability and emission properties of semiconductor core nanocrystals with relatively narrow band gaps.[5] These wide-band-gap semiconductor nanocrystals are also attractive hosts for the formation of doped nanocrystals.[6]

Semiconductor spherical nanostructures, including hollow spheres, solid spheres, and their core/shell structures, have been intensively studied because of their unique properties, which are derived from their special morphologies. Generally, the spherically monodisperse morphology is an important factor in low light scattering at surfaces as well as high packing densities.[7] In particular, hollow nanospheres have potential applications as photonic crystals, delivery vehicle systems, fillers, and catalysts owing to their tailored structural, optical, and surface properties.[8] Enhanced photoluminescence efficiency,[9] improved photon-to-photocurrent charge carrier generation efficiency,[10] and increased conductance[11] have been found in the semiconductor core/shell structures.

Much effort has been devoted to the synthesis of semiconductor spherical nanostructures. However, compared with the significant progress in the preparation of nanospheres of other systems, the formation of monodisperse ZnO,[12] ZnS,[13] and ZnSe nanospheres[14] has been left behind. Reports on the synthesis of well-defined ZnS[15] and ZnSe hollow spheres[16] are still limited, and core/shell structures involving ZnO/ZnS and ZnO/ZnSe have rarely been

* Author to whom correspondence should be addressed. E-mail: jjzhu@netra.nju.edu.cn. Tel and Fax: +86-25-83594976.

† Nanjing University.

‡ Jiangsu Institute of Education.

(1) (a) Pereira, M. F.; Henneberger, K. *Phys. Rev. B* **1998**, *58*, 2064. (b) Pickett, N. L.; Riddell, F. G.; Foster, D. F.; Colehamilton, D. J.; Fryer, J. R. *J. Mater. Chem.* **1997**, *7*, 1855. (c) Kumar, S.; Nann, T. *Small* **2006**, *2*, 316.

(2) (a) Huang, M. H.; Mao, S.; Feick, H.; Yan, H. Q.; Wu, Y. Y.; Kind, H.; Weber, E.; Russo, R.; Yang, P. D. *Science* **2001**, *292*, 1897. (b) Rensmo, H.; Keis, K.; Lindstrom, H.; Sodergren, S.; Solbrand, A.; Hagfeldt, A.; Lindquist, S. E.; Wang, L. N.; Muhammed, M. *J. Phys. Chem. B* **1997**, *101*, 2598. (c) Wang, X. D.; Summers, C. J.; Wang, Z. L. *Nano Lett.* **2004**, *4*, 423. (d) Park, W. I.; Yi, G. C. *Adv. Mater.* **2004**, *16*, 87. (e) Zhao, M. H.; Wang, Z. L.; Mao, S. X. *Nano Lett.* **2004**, *4*, 587.

(3) (a) Park, W.; King, J. S.; Neff, C. W.; Liddell, C.; Summers, C. J. *Phys. Status Solidi B* **2002**, *229*, 949. (b) Bredol, M.; Merichi, J. *J. Mater. Sci.* **1998**, *33*, 471. (c) Calandra, P.; Gofferdi, M.; Liveri, V. T. *Colloids Surf., A* **1999**, *9*, 160. (d) Prevenslik, T. V. *J. Lumin.* **2000**, *87*, 1210.

(4) (a) Matasuoka, T. *Adv. Mater.* **1996**, *8*, 469. (b) Pässler, R.; Griebl, E.; Ripel, H.; Lautner, G.; Bauer, S.; Preis, H.; Gebhardt, W.; Buda, B.; As, D. J.; Schikora, D.; Lischka, K.; Papagelis, K.; Ves, S. *J. Appl. Phys.* **1999**, *86*, 4403. (c) Bonard, J. M.; Ganiere, J. D.; Vanzetti, L.; Paggel, J. J.; Sorba, L.; Franciosi, A.; Herve, D.; Molva, E. *J. Appl. Phys.* **1998**, *84*, 1263.

(5) (a) Hines, M. A.; Guyot-Sionnest, P. *J. Phys. Chem.* **1996**, *100*, 4681. (b) Cao, Y.; Banin, U. *J. Am. Chem. Soc.* **2000**, *122*, 9692. (c) Reiss, P.; Bleuse, J.; Pron, A. *Nano Lett.* **2002**, *2*, 781.

(6) (a) Norris, D. J.; Yao, N.; Charnock, F. T.; Kennedy, T. A. *Nano Lett.* **2001**, *1*, 3. (b) Malik, M. A.; O'Brien, P.; Revaprasadu, N. *J. Mater. Chem.* **2001**, *11*, 2382. (c) Norman, T. J.; Magana, D.; Wilson, T.; Burns, C.; Zhang, J. Z.; Cao, D.; Bridges, F. *J. Phys. Chem. B* **2003**, *107*, 6309.

(7) Kang, Y. C.; Park, S. B.; Lenggoro, I. W.; Okuyama, K. *J. Phys. Chem. Solids* **1999**, *60*, 379.

(8) (a) Caruso, F. *Chem.−Eur. J.* **2000**, *6*, 413. (b) Caruso, F. *Adv. Mater.* **2001**, *13*, 11. (c) Yuan, J. K.; Laubernds, K.; Zhang, Q. H.; Suib, S. L. *J. Am. Chem. Soc.* **2003**, *125*, 4966.

(9) (a) Reiss, P.; Bleuse, J.; Pron, A. *Nano Lett.* **2002**, *2*, 781. (b) Chen, H. S.; Lo, B.; Hwang, J. Y.; Chang, G. Y.; Chen, C. M.; Tasi, S. J.; Wang, S. J. J. *J. Phys. Chem. B* **2004**, *108*, 17119.

(10) Nasr, C.; Hotchandani, S.; Kim, W. Y.; Schwehl, R. H.; Kamat, P. V. *J. Phys. Chem. B* **1997**, *101*, 7480.

(11) Gao, T.; Li, Q. H.; Wang, T. H. *Chem. Mater.* **2005**, *17*, 887.

(12) (a) He, Y. J. *Mater. Lett.* **2005**, *59*, 114. (b) Seelig, E. W.; Tang, B.; Yamilov, A.; Cao, H.; Chang, R. P. H. *Mater. Chem. Phys.* **2003**, *80*, 257.

(13) (a) Zhang, Y.; Li, Y. D. *J. Phys. Chem. B* **2004**, *108*, 17805. (b) Joo, J.; Na, H. B.; Yu, T.; Yu, J. H.; Kim, Y. W.; Wu, F. X.; Zhang, J. Z.; Hyeon, T. *J. Am. Chem. Soc.* **2003**, *125*, 11100. (c) Velikov, K. P.; Van Blaaderen, A. *Langmuir* **2001**, *17*, 4779.

(14) (a) Peng, Q.; Xu, S.; Zhuang, Z. B.; Wang, X.; Li, Y. D. *Small* **2005**, *1*, 216. (b) Shen, G. Z.; Chen, D.; Tang, K. B.; Qian, Y. T. *J. Cryst. Growth* **2003**, *257*, 276.

(15) (a) Ma, Y.; Qi, L.; Ma, J.; Cheng, H. *Langmuir* **2003**, *19*, 4040. (b) Breen, M. L.; Donsmore, A. D.; Pink, R. H.; Qadri, S. Q.; Ratna, B. R. *Langmuir* **2001**, *17*, 903. (c) Gu, F.; Li, C. Z.; Wang, S. F.; Lü, M. K. *Langmuir* **2006**, *22*, 1329. (d) Yin, J. L.; Qian, X. F.; Yin, J.; Shi, M. W.; Zhou, G. T. *Mater. Lett.* **2003**, *57*, 3859. (e) Liu, H. J.; Ni, Y. H.; Han, M.; Liu, Q.; Xu, Z.; Hong, J. N.; Ma, X. *Nanotechnology* **2005**, *16*, 2908. (f) Wolosiuk, A.; Armagan, O.; Braun, P. V. *J. Am. Chem. Soc.* **2005**, *127*, 16356.

(16) (a) Peng, Q.; Dong, Y. J.; Li, Y. D. *Angew. Chem., Int. Ed.* **2003**, *42*, 3027. (b) Jiang, C. L.; Zhang, W. Q.; Zou, G. F.; Yu, W. C.; Qian, Y. T. *Nanotechnology* **2005**, *16*, 551. (c) Wang, X.; Chen, X.; Zheng, H.; Jin, J.; Zhang, Z. *Appl. Phys. A* **2005**, *80*, 511.

10.1021/la701299w CCC: $37.00
Published on Web 08/24/2007

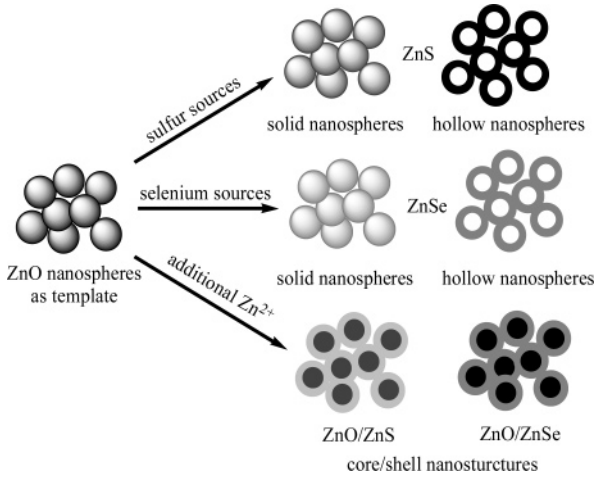

Figure 1. Schematic illustration of the chemical conversion method to a Zn-based semiconductor solid and hollow spheres and their core/shell nanostructures. Through a sonochemical reaction, monodisperse ZnO nanospheres can be obtained. These as-obtained ZnO nanospheres can be further converted to corresponding spherical chalcogenide nanostructures through an ultrasound-assisted substitution reaction at room temperature.

prepared and studied. Therefore, it is desirable to explore diverse routes for the synthesis of spherical Zn-based semiconductor nanostructures with promising novel properties, and methods that may be feasible, easily controllable, and easily repeatable are urgently needed.

In this article, a convenient chemical conversion method that allows the direct preparation of organized nanocrystalline semiconductor solid and hollow spheres as well as their core/shell structures is reported. By using monodisperse ZnO nanospheres as a starting reactant and in situ template, a series of spherical chalcogenide nanostructures have been successfully prepared through an ultrasound-assisted solution-phase conversion process. The chemical conversion mechanism is established in Figure 1.

Commonly used template syntheses for hollow spheres, such as with silica spheres, polymer latex spheres, core/shell gel particles, liquid droplets, and emulsion droplets, are usually suitable for certain specific semiconductor spheres, and after formation, the templates remain in the system and need to be removed later.[13c,17] Compared with those processes, our process is a direct and relatively general synthetic method leading to a significant reduction in fabrication time. Sonication of the precursor in the presence of support materials provides an alternative means of trapping the produced nanoparticles.[18] The optical properties, including photoluminescence (PL) and electrogenerated chemiluminescence (ECL), of the as-prepared nanostructures are investigated.

Experimental Section

Materials. All reagents used were of analytical purity and were used without further purification. $Zn(NO_3)_2 \cdot 6H_2O$, PEG-20000, triethanolamine (TEA), thioacetamide (TAA), and thiourea were purchased from Beijing Chemical Reagents Ltd. Co. of China. Na_2SeO_3, $N_2H_4 \cdot H_2O$, and absolute ethanol were purchased from Shanghai Second Chemical Reagent Factory of China.

(17) (a) Caruso, R. A.; Susha, A.; Caruso, F. *Chem. Mater.* **2001**, *13*, 400. (b) Sun, X. M.; Li, Y. D. *Angew. Chem.* **2004**, *116*, 607. Sun, X. M.; Li, Y. D. *Angew. Chem., Int. Ed.* **2004**, *43*, 597. (c) Putlitz, B.; Landfester, K.; Fischer, H.; Antonietti, M. *Adv. Mater.* **2001**, *13*, 500. (d) Ma, Y.; Qi, L.; Ma, J.; Cheng, H.; Shen, W. *Langmuir* **2003**, *19*, 9079.

(18) (a) Dhas, N. A.; Zaban, A.; Gedanken, A. *Chem. Mater.* **1999**, *11*, 806. (b) Gao, T.; Wang, T. H. *Chem. Commun.* **2004**, 2558. (c) Dhas, N. A.; Gedanken, A. *Appl. Phys. Lett.* **1998**, *72*, 2514.

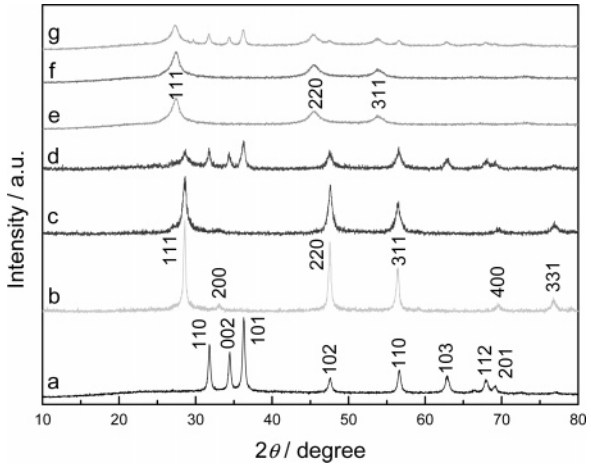

Figure 2. XRD patterns of (a) ZnO spheres, (b) ZnS hollow spheres, (c) ZnS solid spheres, (d) ZnO/ZnS core/shell structure, (e) ZnSe hollow spheres, (f) ZnSe solid spheres, and (g) ZnO/ZnSe core/shell structure.

Synthesis. *ZnO Nanospheres.* $Zn(NO_3)_2 \cdot 6H_2O$ (0.45 g, 0.0015mol) was dissolved in H_2O (100 mL), and then PEG-20000 (1 g) and TEA (2 mL) were introduced sequentially with stirring to form a clear solution. The transparent solution was exposed to high-intensity ultrasound irradiation under ambient air for 30 min. Ultrasound irradiation was generated with a high-intensity ultrasonic probe (Xinzhi. Co., China, JY92-2D, 0.6 cm diameter; Ti-horn, 20 kHz, 60 W/cm^2) immersed in the reaction solution. A white precipitate was centrifuged, washed with distilled water and absolute ethanol in sequence, and finally dried in air. The final products were collected for characterizations and further preparation.

ZnS Hollow and Solid Nanospheres. As-prepared ZnO nanospheres (0.0081 g, 0.001 mol) were well dispersed in 90% EtOH (50 mL) by 5 min of sonication in a normal ultrasonic bath (50 Hz). TAA (0.09 g, 0.0012 mol) or thiourea (0.5 g, 0.006 mol) was dissolved in the above solution. The mixture was exposed to high-intensity ultrasound irradiation for 30 min.

ZnSe Hollow and Solid Nanospheres. The as-prepared ZnO nanospheres (0.0081 g, 0.001 mol) and Na_2SeO_3 (0.173 g, 0.001 mol) were well dispersed in H_2O (40 mL), and then $N_2H_4 \cdot H_2O$ (10 mL) was introduced. The mixture was exposed to high-intensity ultrasound irradiation for 1 h to prepare ZnSe hollow nanospheres. As-prepared ZnO nanospheres (0.0081 g, 0.001 mol) were well dispersed in H_2O (45 mL), and then Na_2SeSO_3[19] (5 mL, 0.2 M) was introduced. The mixture was exposed to high-intensity ultrasound irradiation for 1 h to prepare ZnSe solid nanospheres.

ZnO/ZnS and ZnO/ZnSe Core/Shell Structures. ZnO nanospheres (0.0081 g, 0.001 mol) and $Zn(NO_3)_2 \cdot 6H_2O$ (0.2975 g, 0.001 mol) were well dispersed in EtOH (50 mL), and then TAA (0.09 g, 0.0012 mol) was introduced. The mixture was exposed to high-intensity ultrasound irradiation for 30 min to prepare ZnO/ZnS core/shell structures. ZnO nanospheres (0.0081 g, 0.001 mol) and $Zn(NO_3)_2 \cdot 6H_2O$ (0.2975 g, 0.001 mol) were well dispersed in H_2O (45 mL), and then Na_2SeSO_3[19] (5 mL, 0.2 M) was introduced. The mixture was exposed to high-intensity ultrasound irradiation for 1 h to prepare ZnO/ZnSe core/shell structures.

Characterization. X-ray powder diffraction (XRD) analysis was performed on a Philips X'-pert X-ray diffractometer at a scanning rate of 4°/min in the 2θ range from 10 to 80° with graphite-monochromatized Cu Kα radiation ($\lambda = 0.15418$ nm). The scanning electron micrographs (SEM) were taken on a LEO-1530VP field-emission scanning electron microscope. Transmission electron microscopy (TEM) and selected area electron diffraction (ED) were carried out on a JEOLJEM 200CX transmission electron microscope using an accelerating voltage of 200 kV. High-resolution transmission electron micrographs (HRTEM) were obtained by employing a JEOL-

(19) Zhu, J. J.; Xu, S.; Wang, H.; Zhu, J. M.; Chen, H. Y. *Adv. Mater.* **2003**, *15*, 156.

Table 1. Morphologies and Sizes of the Final Products Synthesized in Different Reaction Systems

reaction systems	products	morphologies	sizes
$Zn(NO_3)_2$ + PEG + TEA	ZnO (hexagonal phase)	solid spheres	400 ± 50 nm
ZnO + TAA	ZnS (cubic phase)	hollow spheres	500 ± 50 nm
ZnO + thiourea		solid spheres	450 ± 50 nm
ZnO + $Zn(NO_3)_2$ + TAA	ZnO/ZnS	core/shell structure	700 ± 50 nm
ZnO + Na_2SeO_3 + N_2H_4	ZnSe (cubic phase)	hollow spheres	500 ± 50 nm
ZnO + Na_2SeSO_3		solid spheres	450 ± 50 nm
ZnO + $Zn(NO_3)_2$ + Na_2SeSO_3	ZnO/ZnSe	core/shell structure	600 ± 50 nm

2010 high-resolution transmission electron microscope with an accelerating voltage of 200 kV. Energy-dispersive X-ray spectroscopy (EDS) analysis was performed during TEM measurements. Photoluminescence spectra (PL) were measured on a SLM48000DSCF/AB2 fluorescence spectrometer made by American SLM Inc. at room temperature.

Cyclic voltammetry (CV) and electrogenerated chemiluminescence (ECL) curves were obtained simultaneously using a model MPI-A electrochemiluminescence analyzer system (Xi'An Remax Electronic Science & Technology Co. Ltd., Xi'An, China). The photomultiplier tube (PMT) used in the above analyzer was held at 800 V during the whole process of detection. Carbon-paste electrodes with a diameter of 4 mm were used as the working electrode.[20] A conventional three-electrode electrochemical cell that was used for all measurements consisted of a carbon-paste working electrode (0.5 cm^2), a Pt wire counter electrode, and a Ag/AgCl reference electrode.

Results and Discussion

Characterization of the Final Products. Figure 2 shows the XRD patterns of the as-prepared products. The obtained ZnO sample is of wurtzite structure (hexagonal phase, space group $P6_3mc$). All of the diffraction peaks in the XRD pattern (Figure 2a) are well assigned to hexagonal-phase ZnO as reported in JCPDS card no. 36-1451. The diffraction peaks of the hollow and solid ZnS spheres (Figure 2b,c) can be indexed to the cubic phase of ZnS with a cell parameter of $a = 5.406$ Å (JCPDS card no. 05-0566). Although the wurtzite phase is the thermodynamically favored bulk form of ZnS, it is very interesting that the product obtained here has a cubic-phase structure. The peaks of spherical ZnSe samples (Figure 2d,e) can be indexed as cubic zinc blende phase ZnSe with a lattice parameter of $a = 5.665$ Å, which is very close to the reported data (JCPDS card no. 05-0522). Cubic phase ZnS and ZnSe are found to coexist with hexagonal phase ZnO in their respective XRD patterns of core/shell structures (Figure 2f,g). The broadening of these diffraction peaks indicates that these samples were composed of nanosized particles.

The summarized morphologies and reaction conditions are illustrated in Table 1, and the representative SEM and TEM images are shown in Figure 3. The as-prepared ZnO sample appeared as uniform solid nanospheres with a diameter of ca. 400 nm, as shown in Figure 3a,b. With these nanoscaled ZnO spheres as a template, hollow and solid spherical ZnS and ZnSe were obtained. When the ZnO template reacted with TAA under ultrasonic irradiation, hollow ZnS spheres with a diameter of ca. 500 nm and a wall thickness of 70−90 nm were obtained (Figure 3c,d). The high-magnification SEM image of one broken sphere reveals the hollow interior (inset of Figure 3c). The surfaces of the hollow spheres are rather rough, indicating that these hollow spheres are composed of small nanoparticles, whereas thiourea substituted TAA as the sulfur source, solid spherical ZnS with a size of 450 nm was produced (Figure 3e,f). ZnSe hollow spheres with a size of ca. 500 nm (Figure 3g,h) were synthesized through the reaction of the ZnO template with Na_2SeO_3 in the presence of hydrazine. Solid ZnSe spheres with a diameter of ca. 450 nm (Figure 3i,j) were prepared via ultrasound treatment of the ZnO and Na_2SeSO_3 suspension. When additional Zn^{2+} ions were introduced into reaction systems, core/shell structures of ZnO/ZnS with a diameter of ca. 700 nm (Figure 3k,l) and ZnO/ZnSe with a diameter of ca. 600 nm (Figure 3m,n) could be fabricated.

The HRTEM images recorded on the shell of the spheres (Figure 4) show that all of the samples are polycrystalline in nature. Interplanar spacings of about 0.31 and 0.27 nm, which correspond to the lattice spacing for the (111) and (200) faces of cubic ZnS, respectively, could be detected in the shell of solid and hollow ZnS spheres as well as in the ZnO/ZnS core/shell structure (Figure 4a−c). The crystal lattice with a lattice spacing of 0.32 nm for the (111) faces of cubic ZnSe is mostly found in the shell of solid, hollow ZnSe spheres and the ZnO/ZnSe core/shell structure (Figure 4d−f).

To further confirm the composition of the prepared products, EDS spectra were recorded for these spheres. Figure 5a is the EDS spectrum from the shell of one broken ZnS hollow sphere, which reveals the presence of Zn and S with an approximate atomic ratio of 1:1.05. The EDS spectrum obtained from the shell of a single ZnSe hollow sphere (Figure 5b) shows the presence of Zn and Se with an approximate atomic ratio of 1:1.14. Parts c and d of Figure 5 show EDS spectra recorded on the outer shell and center of a single ZnO/ZnS sphere, respectively. The shell is composed of Zn and S with an approximate atomic ratio of 1:1.15. However, the EDS spectrum obtained from the center of the sphere shows the presence of Zn, S, and O with an approximate atomic ratio of 1.06:0.13:1, which suggests that the sheath consists of ZnS and the core is mainly ZnO. Parts e and f of Figure 5 are the EDS spectra from the shell and core, respectively, of one ZnO/ZnSe structure with an incomplete package. They both reveal the presence of Zn, Se, and O. However, quantitative analysis shows the approximate atomic ratio of Zn/Se/O to be 1.14:1:0.38 in the shell and 1:0.10:1.21 in the core, respectively. That is, the Se content of the core is much lower than that of the sheath. This suggests that the core is ZnO and that the sheath is mainly composed of ZnSe.

Sonochemical Formation Mechanism. In recent years, ultrasound has become an important tool in chemistry for its application in the synthesis and modification of both organic and inorganic materials.[21] When liquids are irradiated with high-intensity ultrasound, acoustic cavitations (formation, growth, and implosive collapse of the bubbles) provide the primary mechanism for sonochemical effects, during which very high temperatures (> 5000 K), pressures (> 20 MPa), and cooling rates (> 10^{10} K/s) can be achieved upon the collapse of the bubbles.[22] An ultrasound

(20) Ren, T.; Xu, J.; Tu, Y.; Xu, S.; Zhu, J. J. *J. Electrochem. Commun.* **2005**, *7*, 5.

(21) (a) Mdleleni, M. M.; Hyeon, T.; Suslick, K. S. *J. Am. Chem. Soc.* **1998**, *120*, 6189. (b) Gedanken, A. *Ultrason. Sonochem.* **2004**, *11*, 47.

(22) Suslick, K. S.; Choe, S. B.; Cichowlas, A. A.; Grinstaff, M. W. *Nature* **1991**, *353*, 414.

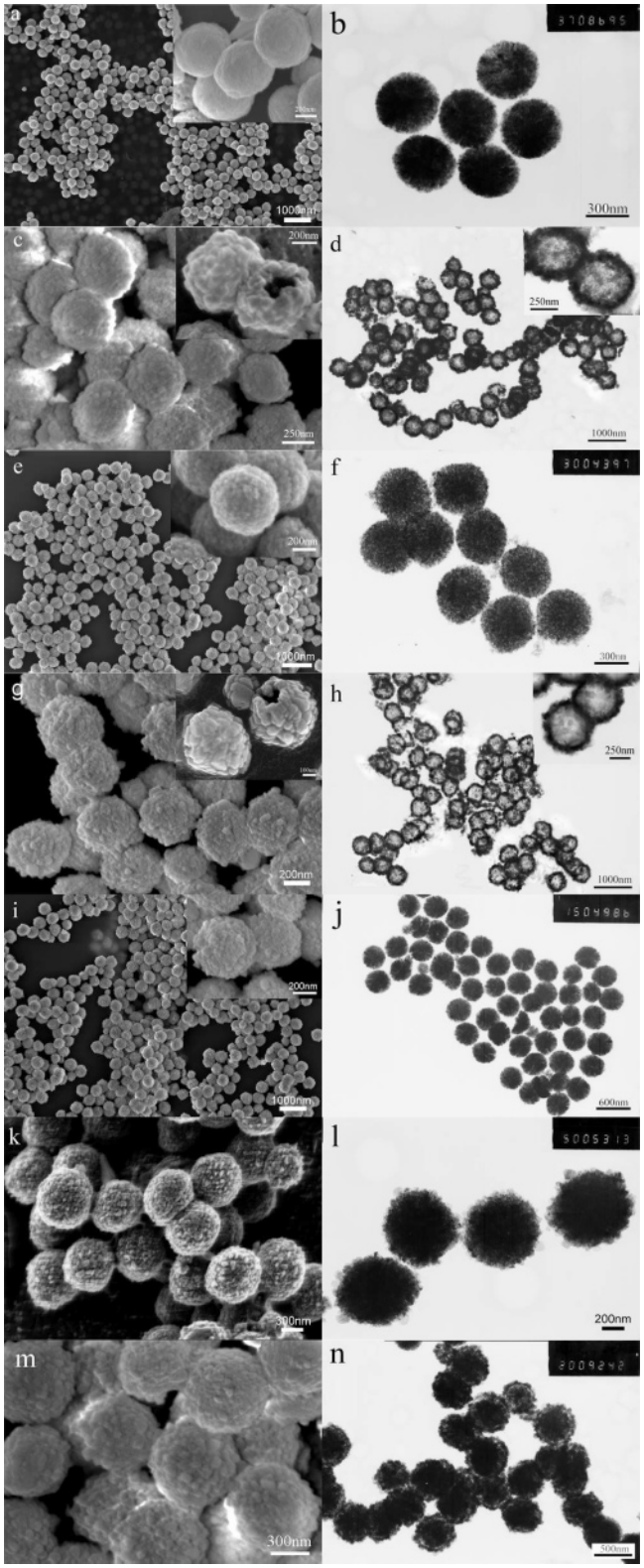

Figure 3. Low- and high-magnification SEM and TEM images of (a, b) ZnO spheres, (c, d) ZnS hollow spheres, (e, f) ZnS solid spheres, (g, h) ZnSe hollow spheres, (i, j) ZnSe solid spheres, (k, l) ZnO/ZnS core/shell structure, and (m, n) ZnO/ZnSe core/shell structure.

wave that is intense enough to produce cavitation can drive chemical reactions such as oxidation, reduction, dissolution, and decomposition.[23]

These reactions can occur in three different regions surrounding the collapse of a bubble in aqueous media.[24] They are the following: (1) the inner environment (gas phase) of the collapsing bubble, where elevated temperatures (several thousands of degrees) and high pressures (hundreds of atmospheres) are produced, causing the pyrolysis of water into H• and OH• and (2) the interfacial liquid region between the cavitation bubbles and bulk solution. The temperature in this region is lower than that of the interior of the bubbles, and the reaction is a liquid-phase reaction; however, the temperature is still high enough to rupture chemical bonds. In addition, greater local hydroxyl radical concentrations in this region have been reported.[25] The third region (3) is the bulk of the solution, which is at ambient temperature and where the reaction between reactant molecules and surviving OH• or H• can still take place. It is generally observed that if the reaction occurs inside the collapsing bubbles then the obtained product is amorphous because of the very high quenching rate experienced by the products. However, if the reaction takes place in the interfacial or bulk region, then one would expect to get crystalline products.[26] In the present case, the sonochemical formation processes of the as-prepared ZnE (E = O, S, Se) nanospheres are probably related to the radical species generated from water molecules by the absorption of ultrasound energy. And because of the nonvolatile nature of Zn^{2+} and the polycrystalline nature of the final products, it appears that the sonochemical reaction occurs within the interfacial region.

The ZnO nanospheres are formed through the sonohydrolysis mechanism, which has been formulated by Gedanken et al.[27] The likely reaction step is

$$Zn^{2+}(aq) + H_2O(l) \rightarrow ZnO(s) + 2H^+(aq) \qquad (1)$$

The probable reaction processes for the sonochemical formation of ZnS and ZnSe nanocrystals in aqueous solution are summarized in Table 2. In the first step, primary radicals are formed by the ultrasound-initiated dissociation of water within the collapsing gas bubbles. In situ generated H• is a highly reducing radical and can react with sulfur or selenium sources to form S^{2-} or Se^{2-}. It is generally accepted that the chemical properties of chalcogens are similar to each other; consequently, S^{2-} or Se^{2-} generated in the solution would have a tendency to be captured by the oxygen vacancies located mainly on the surfaces of ZnO nanospheres.[28] The absorption of S^{2-} or Se^{2-} anions on the ZnO nanospheres provides the initial nucleation sites for the surface growth of ZnS or ZnSe nanoparticles. The sulfur or selenium atoms can diffuse in further from the surface to the inner part of the ZnO nanospheres, resulting in a transition from ZnO to ZnS or ZnSe nanoshperes. Because ZnO spheres are composed of numerous nanocrystals, they exhibit good permeability in solution. Ions and H_2O molecules can therefore move inside the spheres with relative ease, which helps to ensure that the ZnS and ZnSe nanospheres are pure-phase compounds.[14a]

The formation of ZnS and ZnSe hollow spheres may be related to the quick release of intermediate H_2S or N_2 gas (eqs 4 and

(23) (a) Suslick, K. S. *Ultrasound: Its Chemical, Physical and Biological Effects*; VCH: Weinhein, Germany, 1988. (b) Suslick, K. S.; Hammerton, D. A.; Cline, R. E. *J. Am. Chem. Soc.* **1986**, *108*, 5641.
(24) McNamara, W. B.; Didenko, Y. T.; Suslick, K. S. *Nature* **1999**, *401*, 772.
(25) Gutierrez, M.; Henglein, A.; Ibanez, F. *J. Phys. Chem.* **1995**, *95*, 5, 6044.
(26) Jeevanandam, P.; Koltypin, Y.; Gedanken, A.; Mastai, Y. *J. Mater. Chem.* **2000**, *10*, 511.
(27) Kumar, R. V.; Diamant, Y.; Gedanken, A. *Chem. Mater.* **2000**, *12*, 2301.
(28) (a) Yang, P.; Yan, H.; Mao, S.; Russo, R.; Johnson, J.; Saykally, R.; Morris, N.; Pham, J.; He, R.; Choi, H. J. *Adv. Funct. Mater.* **2002**, *12*, 319. (b) Wu, J. J.; Liu, S. C. *Adv. Mater.* **2002**, *14*, 215. (c) Li, Y. B.; Bando, Y.; Golberg, D. *Appl. Phys. Lett.* **2004**, *84*, 3603.

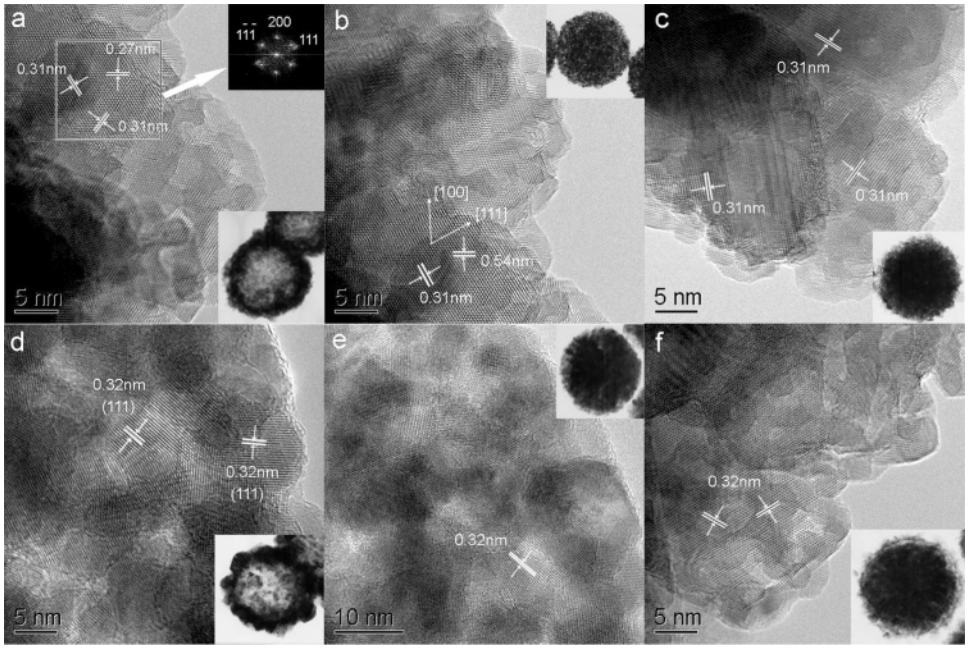

Figure 4. HRTEM images recorded on the shell of (a) ZnS hollow sphere, (b) ZnS solid sphere, (c) ZnO/ZnS core/shell structure, (d) ZnSe hollow sphere, (e) ZnSe solid sphere, and (f) ZnO/ZnSe core/shell structure. The inset of each panel is the corresponding TEM image of the sample.

Table 2. Reaction Processes for the Sonochemical Formation of the ZnS and ZnSe Nanocrystals[a]

ultrasound-initiated dissociation of water	main steps	sulfur or selenium sources	final products
	$H\bullet + OH\bullet + CH_3CSNH_2 \rightarrow CH_3C(NH_2)(OH)-SH$ (3) $H\bullet + OH\bullet + CH_3C(NH_2)(OH)-SH \rightarrow CH_3C(NH_2)(OH)_2 + H_2S$ (4) $CH_3C(NH_2)(OH)_2 \rightarrow CH_3CO(NH_2) + H_2O$ (5) $ZnO + H_2S \rightarrow ZnS + H_2O$ (6) nZnS$\rightarrow$(ZnS)$_n$ (7)	TAA	ZnS hollow nanospheres
$H_2O \rightarrow H\bullet + OH\bullet$ (2)	$2H\bullet + CS(NH_2)_2 \rightarrow H_2S + \bullet C(NH_2)_2$ (8) $ZnO + H_2S \rightarrow ZnS + H_2O$ (9) nZnS $\rightarrow$ (ZnSe)$_n$ (10)	thiourea	ZnS solid nanospheres
	$SeO_3^{2-} + N_2H_4 + 2H\bullet \rightarrow Se^{2-} + 3H_2O + N_2$ (11) $ZnO + Se^{2-} + 2H^+ \rightarrow ZnSe + H_2O$ (12) nZnSe $\rightarrow$ (ZnSe)$_n$ (13)	Na_2SeO_3	ZnSe hollow nanospheres
	$2H\bullet + SeSO_3^{2-} \rightarrow Se^{2-} + 2H^+ + SO_3^{2-}$ (14) $ZnO + Se^{2-} + 2H^+ \rightarrow ZnSe + H_2O$ (15) nZnSe $\rightarrow$ (ZnSe)$_n$ (16)	Na_2SeSO_3	ZnSe solid nanospheres

[a] The formation of H_2S from TAA may follow another route as well: $2H\bullet + CH_3CSNH_2 \rightarrow \bullet CO(NH_2)CH_3 + H_2S$.[11]

11). In the system using TAA as the sulfur source or Na_2SeO_3 as the selenium source, the reaction is faster than for the other two systems, respectively (thiourea and Na_2SeSO_3 systems). The quicker release of the intermediate gas provides higher permeating pressure and faster permeating speed, which results in a faster consumption of ZnO nanospheres and the eventual conversion to hollow spheres. Ostwald ripening may also be responsible for the formation of hollow nanospheres through a solid evacuation and subsequent recrystallization process.[29]

In the case of core/shell structures, the produced S^{2-} or Se^{2-} ions react with additional free Zn^{2+} ions in the solution to form ZnS or ZnSe clusters. When there exists a supporter such as ZnO nanospheres, the sonochemically generated ZnS or ZnSe clusters would be attached on its surface to form a composite nanomaterial with core/shell-type geometry.[18b,c] The last two steps in the reaction could be described as follows:

$$Zn^{2+} + H_2S \rightarrow ZnS + 2H^+ \quad (17)$$

$$n(ZnS) + ZnO \rightarrow ZnO/ZnS \quad (18)$$

$$Zn^{2+} + Se^{2-} \rightarrow ZnSe \quad (19)$$

$$n(ZnSe) + ZnO \rightarrow ZnO/ZnSe \quad (20)$$

To summarize the formation mechanism of these spherical nanocrystals, a schematic illustration is proposed, as shown in Figure 6. This is a simple and relatively general route to the preparation of semiconductor solid and hollow spheres.

PL Study. Figure 7a illustrates the PL spectrum of the spherical ZnO nanostructure under photon excitation of 325 nm. A strong emission at 581 nm in the yellow region, which can be attributed to intrinsic defects in ZnO as oxygen interstitials,[30] dominates

(29) Liu, B.; Zeng, H. C. *Small* **2005**, *1*, 566.

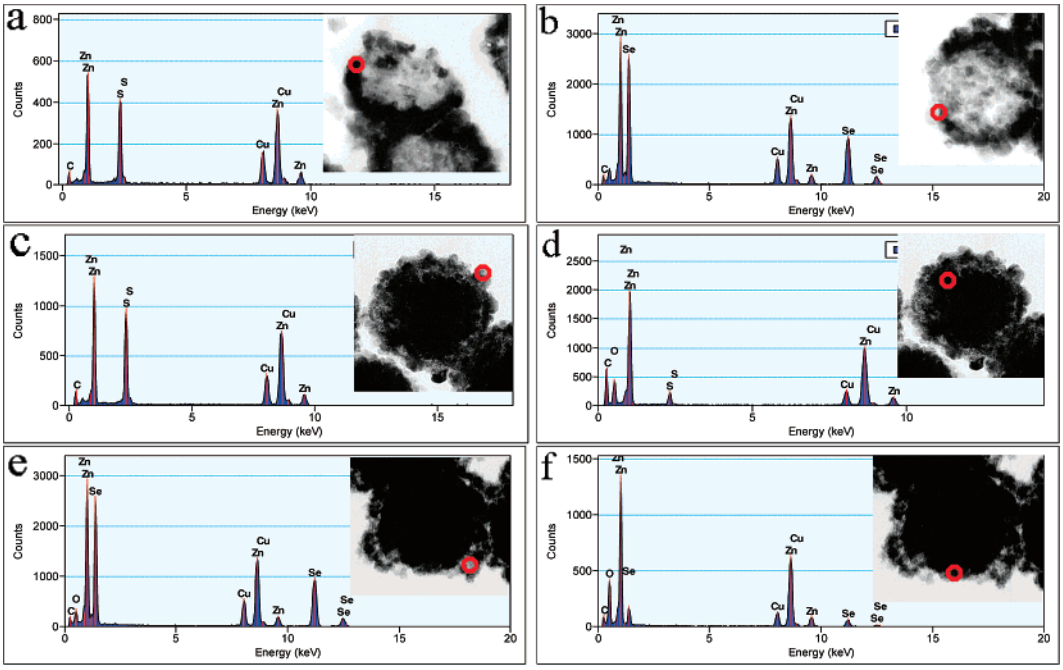

Figure 5. EDS spectra acquired from (a) ZnS hollow sphere, (b) ZnSe hollow sphere, (c, d) ZnO/ZnS core/shell structure, and (e, f) ZnO/ZnSe core/shell structure. (The spectra were obtained from the respective regions, indicated by red circles, in TEM images. The C and Cu lines come from the supporting films and copper grid used for TEM analysis, respectively).

the PL spectrum. One emission band centered at 479 nm has been observed for the solid ZnS nanospheres (Figure 7b), corresponding to the well-known ZnS-related luminescence of zinc vacancies.[31] The PL spectrum of ZnS hollow nanospheres exhibits a strong green emission band centered at 509 nm (Figure 7c). The observable green emission may be derived from some self-activated centers, vacancy states, or interstitial states associated with the peculiar nanostructures.[32,33] A strong blue emission peak at 428 nm accompanied by a weak peak at about 560 nm can be detected in the PL spectrum of the ZnO/ZnS structure (Figure 7d). These emission bands may be caused by the formation of the core/shell structure of the sample.

Figure 8 shows the PL spectra of the as-prepared ZnSe nanocrystals. The main emission bands centered at 420, 450, and 439 nm can be detected for the solid and hollow ZnSe nanospheres and the ZnO/ZnSe core/shell structure, respectively. These emission bands are usually attributed to the edge emission of ZnSe.[34] It is well known that the band gap energy of the bulk ZnSe crystal E_g is 2.67 eV (465 nm).[35] Therefore, the main energy band of as-synthesized ZnSe nanostructures is blue shifted compared with that of bulk materials. The PL spectrum of the core/shell structure also displayed two weak emission peaks located at about 504 and 564 nm, which may be attributed to surface emission and possible metal vacancies.[36]

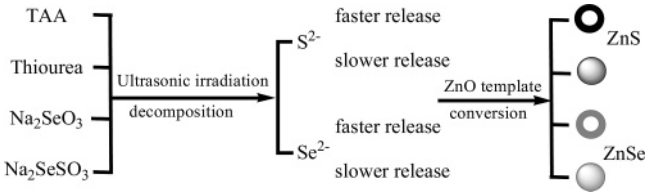

Figure 6. Schematic illustration of the formation mechanism of Zn-based semiconductor spheres.

As shown in Figures 7 and 8, the PL spectra of ZnS and ZnSe hollow spheres displayed enhanced emission intensity compared with that of solid spheres, owing to their hollow structures and large internal surface area of their interior.[37] The integral emission intensity of the two core/shell structures is even higher, which indicates an unusual improvement in the light yield after overcoating. Because the photoluminescence of nanomaterials is sensitive to the synthetic conditions, crystal size, and shape, further investigation is still needed.

Electrogenerated Chemiluminescence Studies. Electrogenerated chemiluminescence (ECL) involves the reaction of electrogenerated species that react to form excited species, usually via an energetic redox reaction.[38] During the past several decades, it has become an important and valuable detection method in analytical chemistry because of its fascinating features, such as high sensitivity, wide linear range, and inexpensive instrumentation.[39] In previous reports, ECL of semiconductor nanocrystals such as Si,[40] Ge,[41] CdS,[20] CdSe,[42] CdTe,[43] and CdSe/ZnSe[44] has been studied, and the results showed that there are electron-transfer reactions that can lead to ECL. However, the ECL property of oxides and other semiconductors has been rarely studied. Herein we describe the ECL of ZnO nanocrystals, and

(30) (a) Dai, L. X.; Chen, L.; Wang, W. J.; Zhou, T.; Hu, B. Q. *J. Phys. Condens. Matter* **2003**, *15*, 2221. (b) Li, D.; Leung, Y. H.; Djurisic, A. B.; Liu, Z. T.; Xie, M. H.; Shi, S. L.; Xu, S. J.; Chan, W. K. *Appl. Phys. Lett.* **2004**, *85*, 1601. (c) Wu, X. L.; Siu, G. G.; Fu, C. L.; Ong, H. C. *Appl. Phys. Lett.* **2001**, *78*, 2285.

(31) (a) Zhang, W. H.; Shi, J. L.; Chen, H. R.; Hua, Z. L.; Yan, D. S. *Chem. Mater.* **2001**, *13*, 648. (b) Rogach, A. L.; Nagesha, D.; Ostrander, J. W.; Giersig, M.; Kotov, N. A. *Chem. Mater.* **2000**, *12*, 2676.

(32) Jiang, Y.; Meng, X. M.; Liu, J.; Xie, Z. Y.; Lee, C. S.; Lee, S. T. *Adv. Mater.* **2003**, *15*, 323.

(33) Mitsui, T.; Yamamoto, N.; Tadokoro, T.; Ohta, S. *J. Appl. Phys.* **1996**, *80*, 6972.

(34) Nazarov, M. V. *Mater. Sci. Eng. B* **2002**, *91*, 349.

(35) Zhu, Z.; Brownlie, G. D.; Thompson, P. J. *Appl. Phys. Lett.* **1995**, *67*, 3762.

(36) Panda, A. B.; Glaspell, G.; El-Shall, M. S. *J. Am. Chem. Soc.* **2006**, *128*, 2790.

(37) (a) Gou, L. F.; Murphy, C. J. *Nano Lett.* **2003**, *3*, 231. (b) Grätzel, M. *Nature* **2001**, *414*, 338. (c) Huynh, W. U.; Dittmer, J. J.; Alivisatos, A. P. *Science* **2002**, *295*, 2425. (d) Nishimura, S.; Abrams, N.; Lewis, B. A.; Halaoui, L. I.; Mallouk, T. E.; Benkstein, K. D.; Lagemaat, J. V.; Frank, A. J. *J. Am. Chem. Soc.* **2003**, *125*, 6306.

(38) For a review, see Faulkner, L. R.; Bard, A. J. In *Electroanalytical Chemistry*; Bard, A. J., Ed.; Marcel Dekker: New York, 1977; Vol. 10.

(39) Fähnrich, K. A.; Pravda, M.; Guibault, G. G. *Talanta* **2001**, *54*, 531.

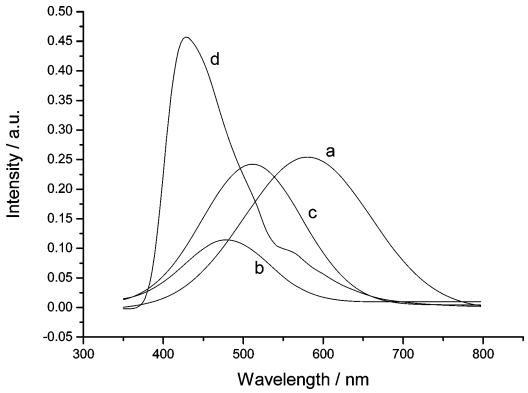

Figure 7. PL spectra of (a) ZnO nanospheres, (b) ZnS solid spheres, (c) ZnS hollow spheres, and (d) ZnO/ZnS core/shell structure.

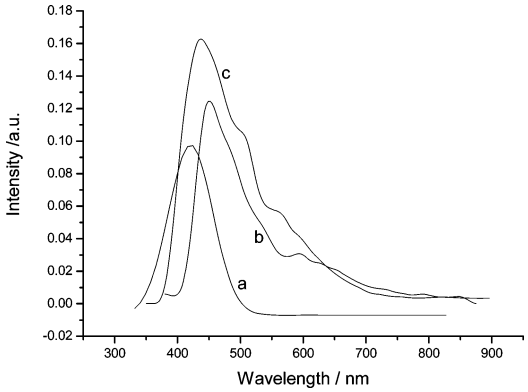

Figure 8. PL spectra of (a) ZnSe solid spheres, (b) ZnSe hollow spheres, and (c) ZnO/ZnSe core/shell structure.

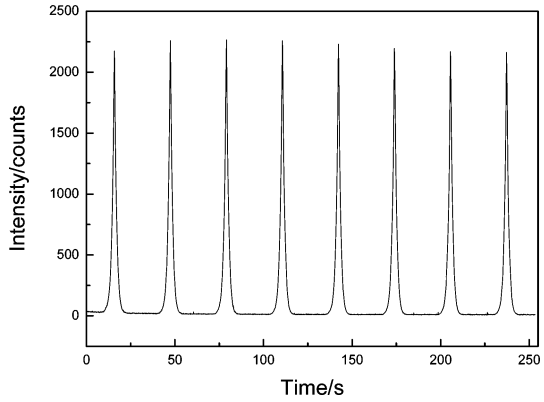

Figure 9. ECL emission from ZnO nanocrystals in 0.1 M $K_2S_2O_8$ + 0.1 M KOH + 0.1 M KCl aqueous solution with potential cycles between 0.1 and −1.5 V (scan rate 100 mV/s).

the as-prepared ZnS, ZnSe, ZnO/ZnS, and ZnO/ZnSe nanocrystals are also studied for comparison.[40]

Figure 9 shows the ECL emission of ZnO nanospheres in 0.1 M KOH and 0.1 M $K_2S_2O_8$ aqueous solution containing 0.1 M KCl as the supporting electrolyte. The electrode potential was cycled between 0.1 and −1.5 V at a scan rate of 100 mV/s. The ECL light emission shows quite good stability and enhanced intensity. ECL is generated by the relaxation of excited-state molecules that are produced through electron-transfer annihilation

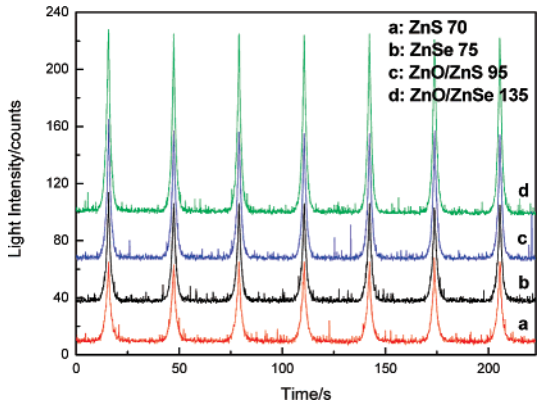

Figure 10. ECL emission from (a) ZnS, (b) ZnSe, (c) ZnO/ZnS, and (d) ZnO/ZnSe in 0.1 M $K_2S_2O_8$ + 0.1 M KOH + 0.1 M KCl aqueous solution with potential cycles between 0.1 and −1.5 V at a scan rate of 100 mV/s. (The numbers on the top right corner of the figure are the respective ECL intensity of final products.)

of electrogenerated anion and cation radicals.[40] As the electrode potential is made more negative, electrons are injected into the ZnO nanocrystals, and electrogenerated anion radicals ($ZnO^{-\bullet}$) are formed. The addition of co-reactants can help overcome either the limited potential window of a solvent or the poor stability of electrogenerated oxidized or reduced species.[40] In our experiments, persulfate was used as the co-reactant. In this case, the reduction of persulfate produces a strong $SO_4^{-\bullet}$ oxidant. This intermediate can react with the negatively charged ZnO nanocrystals to produce excited states and then generate high-intensity light emission.

$$S_2O_8^{2-} + e^- \rightarrow SO_4^{2-} + SO_4^{-\bullet} \quad (21)$$

$$ZnO^{-\bullet} + SO_4^{-\bullet} \rightarrow ZnO^* + SO_4^{2-} \quad (22)$$

The ECL properties of the ZnS, ZnSe, ZnO/ZnS, and ZnO/ZnSe nanocrystals were studied under the same measurement condition as for ZnO (Figure 10). The ECL intensities of these nanocrystals are relatively low as compared with those of the ZnO nanospheres. As proved previously, the ECL emission is much more sensitive to their surface electronic structure than is the PL and is dependent on the surface properties and the presence of surface states.[40,42,44] Therefore, a more detailed investigation of the ECL of these prepared Zn-based semiconductor nanocrystals is urgently needed and is still in progress.

Conclusions

Zn-based II−VI semiconductor nanocrystals have been successfully synthesized via a facile sonochemical route. By using ZnO nanospheres as a template, ZnS, ZnSe solid and hollow nanospheres, and ZnO/ZnS and ZnO/ZnSe core/shell nanostructures have been obtained. The formation mechanism of these nanocrystals is connected to the sonochemical effect of ultrasound irradiation. This method might also have the potential to synthesize other spherical nanostructured functional materials by reacting with appropriate compounds. The PL spectra of the hollow and core/shell nanostructures displayed enhanced emission intensity compared with that of solid spheres. The ECL properties of these semiconductor spheres were researched, for the first time, and the experimental results showed that the nanospheres have interesting photonic properties.

Acknowledgment. We greatly appreciate the support of the National Natural Science Foundation of China for Distinguished

(40) Ding, Z.; Quinn, B. M.; Haram, S. K.; Pell, L. E.; Korgel, B. A.; Bard, A. J. *Science* **2002**, *296*, 1293.
(41) Myung, N.; Lu, X.; Johnston, K. P.; Bard, A. J. *Nano Lett.* **2004**, *4*, 183.
(42) Myung, N.; Ding, Z.; Bard, A. J. *Nano Lett.* **2002**, *2*, 1315.
(43) Bae, Y.; Myung, N.; Bard, A. J. *Nano Lett.* **2004**, *6*, 1153.
(44) Myung, N.; Bae, Y.; Bard, A. J. *Nano Lett.* **2003**, *3*, 1053.

Young Scholars (20325516), the Key Program (20635020), the Creative Research Group (20521503), and the General Program (20575026, 90606016). This work is also supported by the Jiangsu Scientific Foundation of China (BK2006114) and the National Basic Research Program of China (2006CB93301). We thank Professor Yi-Nong Lv from Nanjing University of Technology for his skillful HRTEM measurements.

LA701299W